Wind and Structures, Vol. 14, No. 2 (2011) 167-186
DOI: http://dx.doi.org/10.12989/was.2011.14.2.167

Autorotation of square plates, with application to windborne debris

P. Martinez-Vazquez*[1], M. Sterling[1], C.J. Baker[1], A.D. Quinn[1] and P.J. Richards[2]

[1]*School of Civil Engineering, University of Birmingham, UK*
[2]*Department of Mechanical Engineering, University of Auckland, New Zealand*

(Received April 28, 2010, Accepted October 4, 2010)

Abstract. This paper presents the results of measurements relating to the aerodynamic forces on flat square plates which were allowed to rotate at different speeds about their horizontal axis, by modifying the velocity of the incoming flow. A 1 m square test-sheet and a 0.3 m square test-sheet were fitted with a number of pressure sensors in order to obtain information relating to the instantaneous pressure distribution acting on the test-sheet; a compact gyroscope to record the angular velocity during the rotational motion was also implemented. Previous work on autorotation has illustrated that the angular velocity varies with respect to the torque induced by the wind, the thickness and aspect ratio of the test-sheet, any frictional effects present at the bearings, and the vorticity generated through the interaction between the plate and the wind flow. The current paper sets out a method based on the solution of the equation of motion of a rotating plate which enables the determination of angular velocities on autorotating elements to be predicted. This approach is then used in conjunction with the experimental data in order to evaluate the damping introduced by the frictional effects at the bearings during steady autorotation.

Keywords: autorotation; aerodynamic forces; windborne debris

1. Introduction

Autorotational effects on plates have been explored in the past by a number of authors. In Iversen (1979), previous work, carried out by various researchers on the Magnus Rotor, is described. This includes the identification of lift forces on a rotating cylinder by Gustav Magnus in 1853, as well as its industrial application during the 1920's which encouraged the production of boats and windmills powered by this effect. In Iversen (1979), the difficulties encountered in estimating the magnitude of the Magnus effect during various experiments carried out during four decades (between the 1930's - 1970's) was also described. The rectangular cross section, which was amongst the various sections used for rotors, is where Iversen focused his investigation. He also discussed the influence that vortex shedding and bearing friction have on the tip velocity. Another important contribution of Iversen's work is the correlation made between the plate geometry and mass with tip velocity, which was based on the state of the art of experimental work for rotating and free flying elements,

* Corresponding Author, Research Fellow, E-mail: p.vazquez@bham.ac.kr

including early works from Flachsbart (1932), Dupleich (1941), Bustamante and Stone (1969), Smith (1971), and Glaser and Northup (1971). Given its relevance, Iversen (1979) has been referred in many other studies, including Tachikawa (1983), Baker (2007), and Kordi and Kopp (2009), amongst others. In Tachikawa (1983), further study on autorotating elements was undertaken. In that paper, a series of plates of different dimensions were tested in a wind tunnel and the corresponding force coefficients were determined. Although Tachikawa's experiments covered a smaller range of plate's geometry and mass in comparison to Iversen's work, these helped in the solution of the equations of motion for free flight, which have direct application to windborne debris. In his model, Tachikawa (1983) identified the controlling parameters for free flight, including what we refer to as the Tachikawa Number – see Holmes *et al*. (2006a). Tachikawa's experimental and analytical work has been continued by other researchers, for example Wang and Letchford (2003), Lin *et al*. (2006), Holmes *et al*. (2006b), Baker (2007), Richards *et al*. (2008), and Martinez-Vazquez *et al*. (2009, a, b, c). The motivation of the present investigation is thus to provide further insight into plate autorotation. This has been achieved through extending existing results obtained by using simplified approaches for estimating tip velocities in order to determine data series in the time domain so that the angular motion of plates could then be observed in detail. Obtaining time series of pressure would shed additional light on the study of autorotational motion of plates, and also it would enable further studies to be undertaken in the future, for example applying spectral and modal decomposition techniques. The present investigation explores the phenomenon of autorotation from an analytical and experimental perspective in order to combine these into an experimental-based formulation, thus making sure that the final conclusions of the study are based on physical and theoretical evidence. The experimental information was obtained from a series of tests carried out on two tests-sheets of different size (1 m square and 0.3 m square) using a novel acquisition system which involves pressure transducers mounted within the test plates, see Martinez-Vazquez *et al*. (2009b, c). The angular motion of the plates was measured using a gyroscope which was fitted within the test-sheets. Pressure transducer and gyroscope data was recorded on a data acquisition system within the test plates that enabled logging data in real time by using a portable card. The analytical part of the study combines the experimental results with previous studies by Iversen (1979) and Tachikawa (1983) outlined above, in order to provide simple expressions to estimate the input torque induced by the wind flow as well as the frictional effects at the bearings.

The paper has been organised in the following way: section 2 deals with the experimental arrangements, while sections 3 shows the experimental results for autorotating tests. Section 4 introduces the analytical model for the computation of autorotational motion in the time domain and proposes a method for assessing frictional damping, in addition to presenting a qualitative comparison to Iversen's model through a parametric study. Finally, section 5 discusses the results and draws appropriate conclusions.

2. Experimental set-up

The present work is based on the same experimental setting described in Martinez-Vazquez *et al*. (2009b, c). Therefore, only the main aspects which are relevant to the present case are given below. The test-sheets, representing typical roof cladding panels, were made of polystyrene. There were two sizes: 1 m square and 0.3 m square, both of which are 2.5 cm thick. The large and small test-sheets weighed 2.7 kg and 1 kg respectively. As illustrated in Fig. 1, the larger test-sheet contained

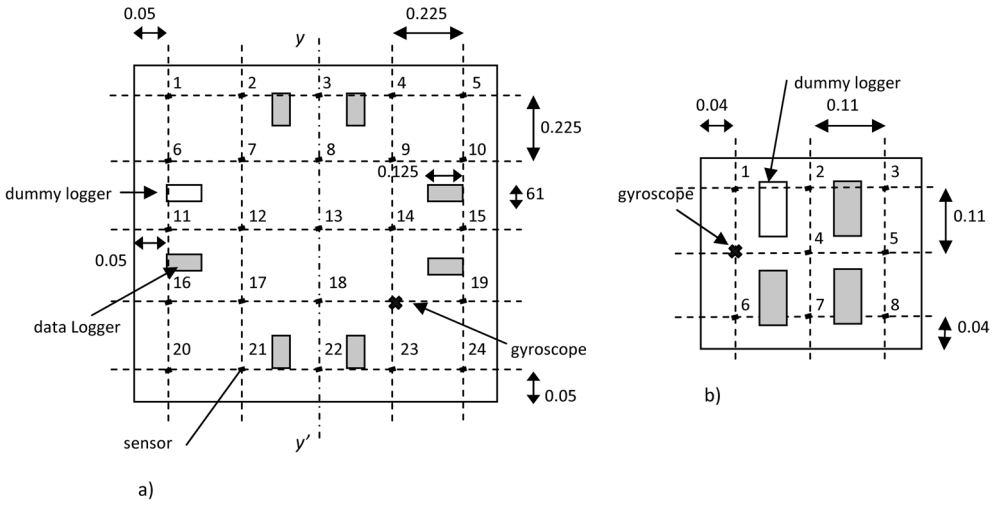

Fig. 1 Logging system configuration on (a) 1 m square and (b) 0.3 m square test-sheet (all dimensions in m)

24 pressure sensors, 7 data loggers and 1 gyroscope, while the smaller test-sheet contained 8 sensors, 3 data loggers, and 1 gyroscope. Differential pressure transducers manufactured by Sensortechnics with output voltage and pressure acceptance in the range of 0.25 - 4.5 V and 0 - 2.5 mbar, respectively, were used. The gyroscope is part of an analog inertial measurement unit (*AccelRate3D*) manufactured by Omni instruments. The maximum acceleration capacity and rate of rotation are 10 g and 600 / sec respectively. The unit requires a 5 V direct current supply during operation. For the data logger the portable card *XR440-M* manufactured by Omni instruments was considered suitable to work in combination with the sensors and gyroscope. One data logger supports 4 pressure sensors or one gyroscope, accepts an input signal of 0 - 5 V and it provides a resolution of 12 bits with a maximum sampling frequency of 200 Hz. The general characteristics of the two experimental test-sheets are shown in Fig. 1.

The supporting system for the test-sheets (Fig. 2) consisted of two metallic frames of height 1.5 m. Each support had a vertical plate at the top extreme where an aluminium frame, which was attached to the test-sheets, could be inserted using a pin connector. This is shown in Fig. 2 - Det. A where it can be observed that there was direct contact between the pin connector supporting the test-sheet and the vertical plate. The same bearing system was used for all tests discussed in the

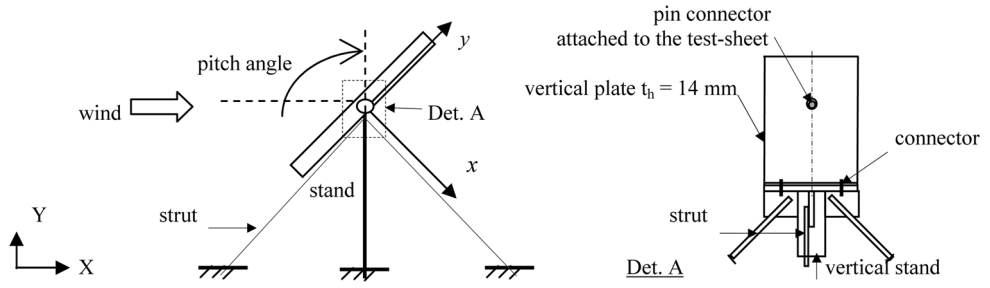

Fig. 2 Bearing (lateral view) system used in all tests

following sections. During the tests, rotation around the z axis was permitted whilst any other degree of freedom remained restricted. The experiments were carried out in the twisted flow wind tunnel at the University of Auckland in New Zealand (for further details see Martinez-Vazquez *et al*. 2009b, c). Uniform wind speeds U = 5, 7.5, and 10 m/s were selected for the autorotational tests on the 1 m square specimen. Initial experiments indicated that at U = 5 m/s, the smaller test-sheet did not undergo a steady autorotation due to high friction at the bearings – in section 4, it will be shown however, that under lower levels of friction the plate would autorotate. Hence, the results presented below relate to U = 7.5 and 10 m/s. In all cases, the test duration was of 30 s for each static experiment, with a sampling frequency of 10 Hz. The corresponding experimental period and sampling frequency for the auto-rotating tests was ~120 s and 200 Hz respectively.

3. Autorotational tests

During testing, each plate was released at a pitch angle of about 15° from its horizontal position. The pitch angle is formed between the test-sheet and a horizontal plane, increasing its value with the torque. The angular velocity $(\dot{\varphi})$ during autorotational motion was measured using a gyroscope. These measurements allowed the establishment of the relationship between the time and the angular coordinate (φ) for the test-sheets during a cycle which is shown in Fig. 3 for measurements taken at U = 7.5 m/s for a normalised period which dimensionless fractions are given by t / T_0 - where t is the time and T_0 is the period of the characteristic cycle. Note that the relationship between φ and t / T_0 represented in this figure is not unlike the one assumed in Martinez-Vazquez *et al*. (2009c) for the large test-sheet where no gyroscope had been implemented in the experimental setting.

It can be seen in Fig. 3 that larger fluctuations of velocity within a cycle were observed on the large test-sheet. This is illustrated in more detail through a typical 5-second series in Figs. 4 and 5 for the large and small test-sheet, respectively. The selected time intervals (90 s $\leq t \leq$ 95 s) were extracted from the last 30 seconds of autorotational tests (steady autorotation) which lasted approximately 107 sec. Note that in both cases, the peak velocities vary from one half-cycle to another (one peak on the plots correspond to a half-cycle) which is more clearly observed for the small test-sheet.

The amplitude of the angular velocity fluctuation under steady autorotation was measured in terms

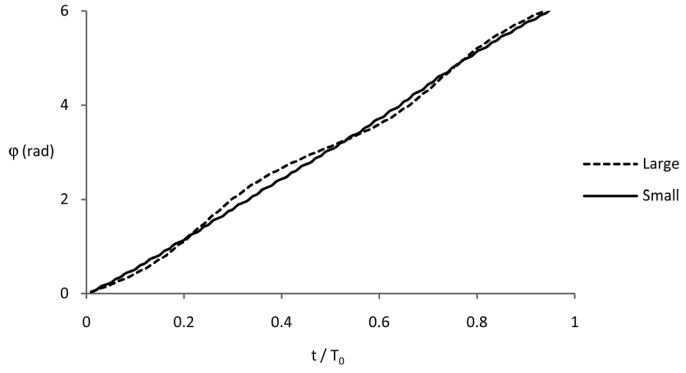

Fig. 3 Relationship between dimensionless time and angular position - large and small test-sheets for U = 7.5 m/s

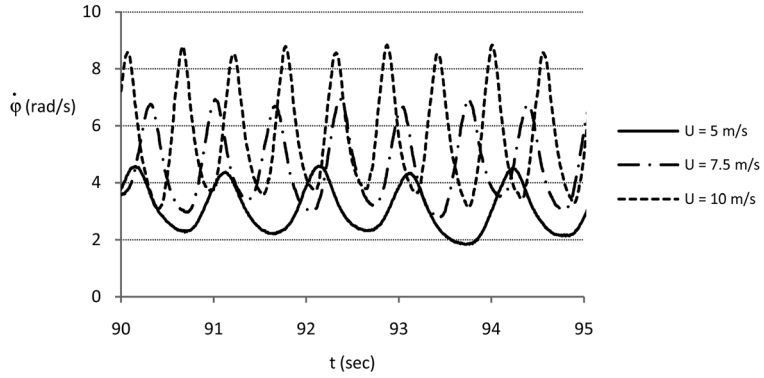

Fig. 4 Fluctuation of angular velocity during steady autorotation – large test-sheet for U = 5, 7.5 and 10 m/s

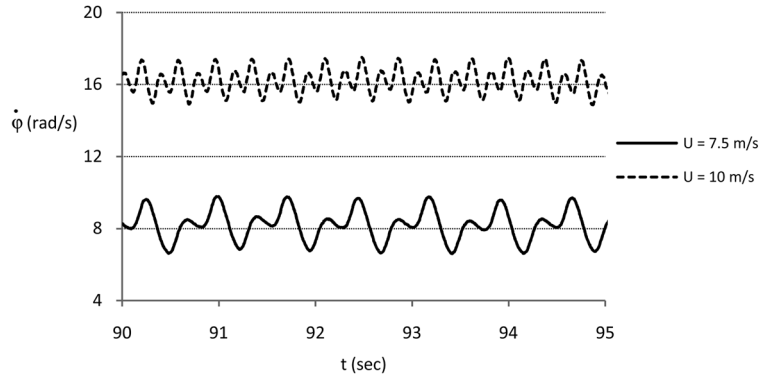

Fig. 5 Fluctuation of angular velocity during steady autorotation – small test-sheet for U = 7.5 and 10 m/s

of the index of variation (I_v) defined as the ratio of the standard deviation of $\dot{\varphi}$ to the corresponding mean value. For the large test-sheet, I_v was estimated to be of about 0.27, 0.28 and 0.31, for U = 5, 7.5 and 10 m/s, respectively. The corresponding values for the small test sheet were 0.10 and 0.04 for U = 7.5 and 10 m/s, respectively, i.e., whilst I_v appears to increase with the wind velocity for the large test-sheet, the opposite was observed for the small one, which seems to be largely due the variability of frictional effects at the bearings – see Appendix A. It will be shown in the following section that the index of variation would ideally be a constant fraction of $\dot{\varphi}$ for the same plate during steady autorotation, i.e., no variation with the wind speed.

The computation of instantaneous forces on the test-sheets was achieved through an integration of the net pressure coefficients per cycle which were then averaged. The normal forces could be computed for every angle after establishing the relationship between the time and the angular position as explained above. In this way the force coefficients were observed at every cycle and their average defined a characteristic period. The characteristic periods for the large and small test-sheet are shown in Fig. 6.

Fig. 6 shows the variation of the force coefficient with respect to time (i.e., the pitch angle). In general, the peak values of C_N for the large test-sheet are in good agreement with those presented in Martinez-Vazquez *et al*. (2009c) for the same specimen. There is however a slight difference with

regard to the characteristic periods, which for the previous experiment (referred to as *L1*) are 2.36 s, 1.48 s, and 1.12 s for $U = 5$, 7.5, and 10 m/s respectively. For the present experiment (*L2*) the periods computed are 2.06 s, 1.36 s, and 1.11 s for the same wind velocities. The differences, in the order listed are of about 14 %, 8 %, and 1%, respectively. In Appendix A, it will be shown that, given the various factors that influence the process of estimation of the rotational periods, the differences found in these two experiments are within expected limits. This figure also shows the characteristic cycles for the small test-sheet. In this case the peak values of C_N were around $\pm$ 2 and the periods are 0.752 s, and 0.39 s for $U = 7.5$ and 10 m/s, i.e., the results are significantly different from those found on the larger test-sheet.

Fig. 7 shows a comparison of the normal force coefficients for the two test-sheets using normalised periods of rotation. This representation has enabled the variations of the values of C_N at equivalent instants of normalised time to be observed. It is noticeable the asymmetry of the relative differences amongst data from the large and small test-sheets between half-cycles. Such differences might correspond to the variations of the angular velocity registered by the gyroscope as shown in Figs. 4 and 5.

The results presented above were used to determine the average tip velocities under steady autorotation given in Table 1 for the two test-sheets. The corresponding values from the experimental work reported in Martinez-Vazquez *et al*. (2009c) for the large test-sheet (*L1*) are also provided for comparison. The data contained in Table 1 are used in the study described in the next section, where an analytical model is introduced to estimate the tip velocity of autorotating plates.

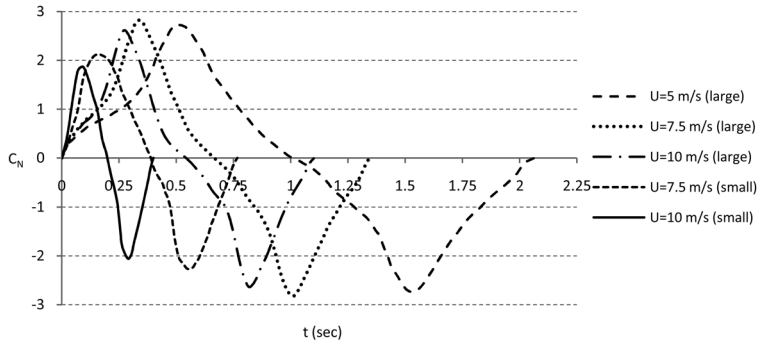

Fig. 6 Normal force coefficients for the large and small test-sheet - characteristic cycles

Fig. 7 Normal force coefficients for the large and small test-sheet - characteristic normalised cycles

Table 1 Tip velocity under steady autorotation for the large and small test sheets

	Large test-sheet *(L1)*			Large test-sheet *(L2)*			Small test-sheet	
	$U = 5$	$U = 7.5$	$U = 10$	$U = 5$	$U = 7.5$	$U = 10$	$U = 7.5$	$U = 10$
$(v / U)_{steady}$	0.265	0.283	0.280	0.304	0.307	0.283	0.166	0.240

4. Analytical model of autorotation

4.1 Tip Velocity

The estimation of the tip velocity *(v / U)* of autorotating plates has been formulated in the past based on experimental observations. In Tachikawa (1983) and Iversen (1979), methods to estimate the ratio $(v / U)_{steady}$ have been suggested. Tachikawa (eq. (1)) gives a constant value for $(v / U)_{steady}$ for aspect ratios *(A)* of 1 and 2 - where $A = b / L$. i.e., the ratio of the width *(b)* and the chord length *(L),* and for thickness ratio t, defined as t_h / L – where t_h represents the plate's thickness, in the range of 0.029 to 0.056.

$$(v / U)_{steady} = 0.32; \text{ for } A = 1,\ 0.029 \leq \tau \leq 0.056 \tag{1a}$$

$$(v / U)_{steady} = 0.48; \text{ for } A = 2,\ \tau = 0.029 \tag{1b}$$

$$(v / U)_{steady} = 0.45; \text{ for } A = 2,\ \tau = 0.053 \tag{1c}$$

Iversen's approach (eq. (2)) accounts for the influence of the aspect ratio *(A);* the thickness parameter (τ); and the inertia parameter *(K)* defined as $I / \rho L^4 b$, where I is the mass moment of inertia. This formulation is based on experimental data by Dupleich (1941), Bustamante and Stone (1969), Smith (1971), and Glaser and Northup (1971), covering a range of values for A and τ which fall in the interval 1 – 4 and 0.0054 – 0.5, respectively.

$$(v / U)_{steady} = f(A) f(\tau) f(K) \tag{2a}$$

$$f(A) = \left[\left(\frac{A}{2 + (4 + A^2)^{1/2}} \right) \left(2 - \left(\frac{A}{A + 0.595} \right)^{0.76} \right) \right]^{2/3} \tag{2b}$$

$$f(\tau) = 0.33 Ln\left(\frac{1}{\tau}\right) - 0.025 \left(Ln\left(\frac{1}{\tau}\right) \right)^2 \tag{2c}$$

$$f(K) \sim 0.8 + \frac{0.2(Ln(K) - Ln(0.1))}{Ln(10) - Ln(0.1)} \tag{2d}$$

Eq. (2d) has been inferred from Iversen (1979) by extrapolating to a value minimum value of K of 0.1 in order to include the value of $K \sim 0.2$ corresponding to the experimental cases reported in the present paper and assuming the difference of 20% between $(v / U)_{K=10}$ and $(v / U)_{K\sim0.22}$ as suggested by Iversen (1979). In Iversen's original work the minimum value of K was approximately

0.22 and corresponded to the minimum value at which steady autorotation was observed in the experimental work reported by Glaser and Northup (1971).

4.2 Numerical model

In Iversen (1979), a method to compute the tip velocity of flat plates was suggested. It consisted of the numerical integration of Eq. (3) below which relates the angular coordinate (φ) to an external torque $T(\varphi)$, moment of inertia I and the damping D_0 which includes bearing friction.

$$I\ddot{\varphi} + D_0\dot{\varphi} = T(\varphi) \tag{3}$$

Iversen derived the following equation for torque, based on the experimental data reported in Smith (1971)

$$T(\varphi) = B[\sqrt{2}\sin(2\varphi + 3\pi/4) - 1] \tag{4}$$

where B is a variable that defines the amplitude of the torque and it must have a negative value in order to obtain positive torque – see Fig. 8. This leads to the following dimensionless equation

$$\left(\frac{L}{2U}\right)^2\frac{d^2\varphi}{dt^2} + \frac{C_U}{K}\frac{L}{2U}\frac{d\varphi}{dt} + \sqrt{2}\frac{C_B}{K}sin(2\varphi + 3\pi/4) = \frac{C_B}{K} \tag{5a}$$

where

$$C_B = \frac{2B}{\rho U^2 bL^2};\ C_U = \frac{4D_0}{\rho UbL^3};\ K = \frac{I}{\rho L^4 b} \tag{5b}$$

Eq. (5) has been transcribed from Iversen (1979). However the parameters C_B and C_U as quoted appear to be incorrect. From Eq. (5a) it can be demonstrated that the values of these variables should be:

$$C_B = \frac{B}{4\rho U^2 bL^2};\ C_U = \frac{D_0}{2\rho UbL^3} \tag{6}$$

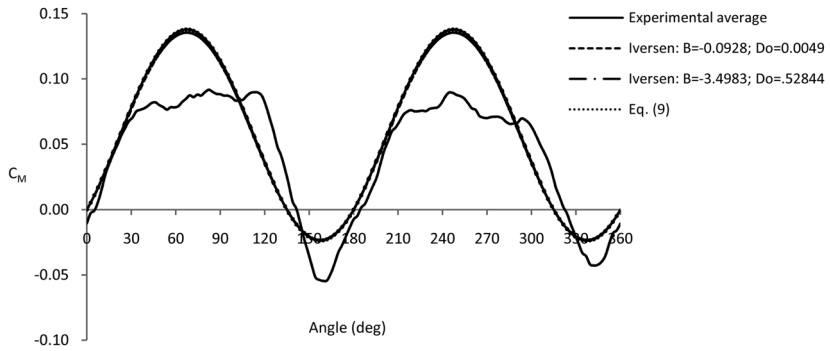

Fig. 8 Moment coefficient inferred from the input torque suggested by Iversen's and experimental data

The practical limitation of the numerical model outlined above is that the input moment and the aerodynamic damping are both unknowns, i.e., the solution of Eq. (5) requires knowledge of the variables B and D_0. According to Iversen's formulation C_B / C_U corresponds to the *lim (v / U)* when $t \to \infty$, i.e., C_B / C_U matches the tip velocity under steady autorotation. In Iversen's treatise the quotient C_B / C_U was iteratively adjusted until the value of rotational speed in Eq. (5a) matched the experimental data reported in Glaser and Northup (1971) in order to estimate the influence of the inertia parameter on $(v / U)_{steady}$.

4.3 Analytical model

The analytical model suggested in the present investigation is based on an approximate solution of Eq. (3) which is given by Eq. (7).

$$\dot{\varphi} = Ce^{\frac{-D_0 t}{I}} + \frac{T(\varphi)}{D_0} \tag{7a}$$

$$C = \dot{\varphi}(0) - \frac{T(\varphi)}{D_0} \tag{7b}$$

It is proposed here that $T(\varphi)$ can be estimated by using the experimental moment coefficients reported in Martinez-Vazquez *et al*. (2009c) for the large test-sheet for three wind velocities, i.e., U = 5, 7.5 and 10 m/s. In that paper, the moment coefficient, defined as $C_M(\varphi) = T(\varphi) / (\rho U^2 L^3/2)$ was given at discrete values within the range of angles $0^o \leq \varphi \leq 360^o$.

On the assumption that $T(\varphi)$ is inferred from $C_M(\varphi)$ as suggested above, the variable D_0 in Eq. (7) would represent the frictional effects at the bearings. It is hypothesised here that any other source of damping would be implicit in $T(\varphi)$. In what follows, the input torque suggested in Iversen (1979), i.e., Eq. (4) and the input torque inferred from the experimental measurements will be referred to as $T(\varphi)_{iversen}$ and $T(\varphi)_{exp}$, respectively.

One important characteristic of $C_M(\varphi)$ inferred from $T(\varphi)_{iversen}$ can be established by using the definition $(v / U)_{steady} = L\dot{\varphi} / 2U$ and the fact that the quotient C_B / C_U matches the *lim (v / U)* when $t \to \infty$, as described in the previous section. This enables the relationship $B / D_0 = \dot{\varphi}$ to be obtained. Hence, the pair (B, D_0) can take an infinite number of values for one particular solution. If two suitable combinations of B and D_0 can result in the same $C_M(\varphi)$ after normalising $T(\varphi)$, it follows that $T(\varphi)_{iversen}$ and $T(\varphi)_{exp}$ can then be combined through the moment coefficient. This is achieved from the definition given by eq. (8) which represents the mean value of eq. (4) over a cycle considering B = 1. A continuous function within the interval $0 \leq \varphi \leq 2\pi$ for the moment coefficient can thus be given through Eq. (9) by letting B = -0.0571 which corresponds to the average value of the experimental moment coefficient computed over a cycle. Note that the sign of B must be negative in Eqs. (4) and (9) in order to obtain positive torque.

$$-1 = \frac{1}{2\pi}\int_0^{2\pi} [\sqrt{2}\sin(2\varphi + 3\pi/4) - 1] \tag{8}$$

$$C_M(\varphi) = -0.0571[\sqrt{2}\sin(2\varphi + 3\pi/4) - 1] \tag{9}$$

Fig. 8 shows a comparison of the moment coefficients for the various cases described above. The experimental average was obtained by using the experimental data reported in Martinez-Vazquez *et al*. (2009c). There are two curves inferred from Iversen's numerical model, which despite the different values for the pair (B, D_0), resulted in an almost identical moment coefficient. The figure also includes the corresponding values obtained through Eq. (9). The difference in the last three cases is however very small and cannot be appreciated at the scale represented on the plot.

Eq. (7) has thus been used to reproduce the experimental results from Glaser and Northup (1971) (presented in Iversen, 1979) using the two approaches described above for the input torque, i.e., $T(\varphi)_{Iversen}$ and $T(\varphi)_{exp}$. Since values for C_B and C_U are given in Iversen's paper (C_B = 0.031and C_U = 0.07216), $T(\varphi)_{iversen}$ can be calculated using Eqs. (4) and (6). The tip velocity for a group of plates with inertia parameters within the range of 0.25 - 10 with an aspect ratio A of 0.5 and thickness parameter τ = 0.0156 was estimated. A damping coefficient of 0.276 kg-m^2/rad-sec was inferred from C_B and C_U. In addition, two more damping values: D_0 = 0.31, 0.35 were used in order to observe the model's sensitivity to variations of this parameter. The tip velocity computed at a range of values K = 0.3, 1, 5, 10, using Iversen's close-form approximation (Eq. (2)) has also been represented in Fig. 9.

In this example, only eq. (2) matches the experimental data at high values of the inertia parameter (K = 10) and, on average, it gives the closest approximation elsewhere. Eq. (7) overestimates the value of v / U at K = 10 by 6% either using $T(\varphi)_{Iversen}$ or $T(\varphi)_{exp}$, for the same damping coefficient D_0 = 0.276. As the value of the damping parameter was increased (i.e., to 0.31 and 0.35), $(v / U)_{steady}$ was underestimated by between 5% - 16%. The best approximation to the experiment of Glaser and Northup (1971) was obtained with a damping coefficient D_0 = 0.31.

The above analysis has illustrated the importance of establishing a reliable method in order to evaluate the damping generated by bearing friction. This can be achieved by using the definition of steady tip velocity suggested in either Tachikawa (1983) or Iversen (1979), which are given here in eqs. (1) and (2), respectively. From Eq. (7) it can be seen that as $t \to \infty$, the angular velocity $\dot{\varphi}$ converges to $T(\varphi) / D_0$ which when combined with the two definitions: $C_{M\text{-}average} = T_{average} / (\rho U^2 L^3 / 2)$ and $(v / U)_{steady} = L\dot{\varphi} / 2U$ leads to equation (10) below.

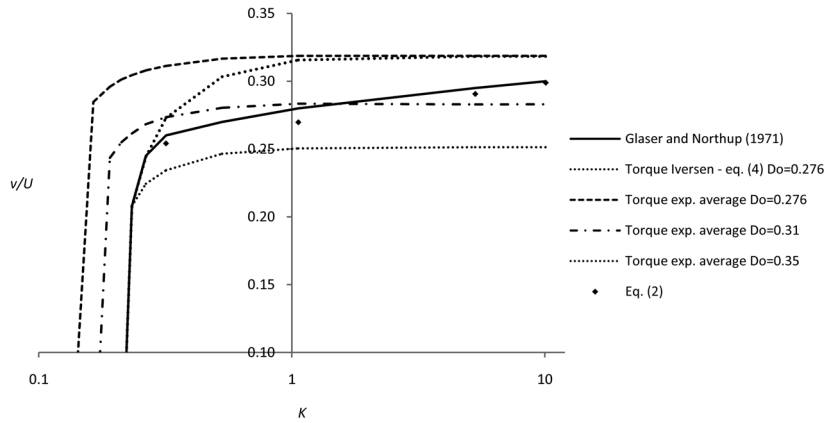

Fig. 9 Variation of the tip velocity with K - various input torque and experimental data by Glaser and Northup (1971) (taken from Iversen (1979)) for a plate with A = 0.5, τ = 0.0156, C_B = 0.031, and C_U = 0.07216

$$(v/U)_{steady} = \frac{C_M - average\ \rho U L^4}{4D_0} \tag{10}$$

It is proposed here to use the following equation for the estimation of the frictional damping taking $C_{M\text{-}average}$ of 0.0571 and using either Eq. (1) or (2) to determine $(v / U)_{steady}$

$$D_0 = \frac{0.0571 \rho U L^4}{4(v/U)_{steady}} \tag{11}$$

4.4 Application of the proposed method

The analytical model set out above is expressed by Eqs. (7) and (11) together with a suitable assumption for torque variation with rotational angle. In what follows, these equations are used to determine the tip velocity of the idealised large and small test-sheets described in Section 2 and the results obtained are presented in Table 2, Figs. 10 and 11. Note that the results for the small test-sheet submitted to $U = 5$ m/s have been included here. The small test-sheet did not undergo autorotation during testing, apparently due to high friction at the bearings - see Section 3, however, the analytical model does predict steady autorotation for this plate, for the levels of friction estimated with eq. (11). The simplified approaches suggested by Iversen (1979) and Tachikawa (1983), also predict steady autorotation for that specimen, which is shown in Table 2 where the tip velocity computed using all those approaches is compared. The experimental results measured in the wind tunnel - see Table 1, as well as the damping due to bearing friction and thickness parameters involved in those calculations are all shown in Table 2. In this table, the experimental damping due to bearing friction $(D_{0\text{-}exp})$, inferred by using Eq. (11) and the experimental tip velocity, has also been included. It can be seen that the values of $D_{0\text{-}exp}$ are consistently higher than the theoretical predictions. Those values also show that the variability of $D_{0\text{-}exp}$ from one test to another, i.e., between the results given for *L1* and *L2*, is of the order of 0.079, on average, which is within the uncertainty bounds estimated for bearing friction - see Appendix A.

The results given by the analytical model are encouraging and show small differences of

Table 2 Estimation of $(v / U)_{steady}$ through several approaches

		Large test-sheet *(L1)*			Large test-sheet *(L2)*			Small test-sheet			
		$U = 5$	$U = 7.5$	$U = 10$	$U = 5$	$U = 7.5$	$U = 10$	$U = 5$	$U = 7.5$	$U = 10$	m/s
	D_0*	0.264	0.396	0.528	0.264	0.396	0.528	0.0025	0.0037	0.0050	Eq. (11)
	$D_{0\text{-}exp}$*	0.329	0.463	0.624	0.288	0.427	0.618	-	0.0064	0.0060	
	τ	0.025	0.025	0.025	0.025	0.025	0.025	0.0847	0.0847	0.0847	
a)	$(v / U)_{steady}$	0.317	0.318	0.317	0.317	0.318	0.317	0.258	0.258	0.258	Eqs. (7, 9 and 11)
b)	$(v / U)_{steady}$	0.331	0.331	0.331	0.331	0.331	0.331	0.284	0.284	0.284	Iversen, 1979
c)	$(v / U)_{steady}$	0.320	0.320	0.320	0.320	0.320	0.320	0.320**	0.320**	0.320**	Tachikawa, 1983
d)	$(v / U)_{steady}$	0.265	0.283	0.280	0.304	0.307	0.283	-	0.166	0.240	Experimental
	a) / d)	1.19	1.12	1.13	1.04	1.03	1.12	-	1.55	1.07	

(*) kg-m^2/rad-sec; (**) In Tachikawa (1983) $0.029 \leq \tau \leq 0.056$ for $A = 1$

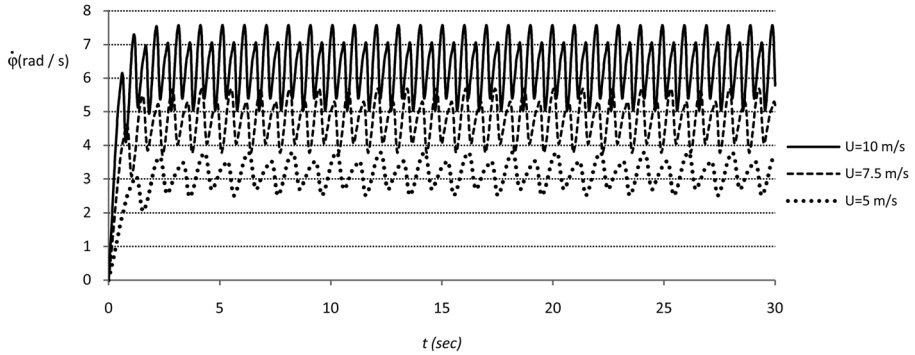

Fig. 10 Time history of angular velocity given by Eq. (7) - large test-sheet, U = 5, 7.5, and 10 m/s

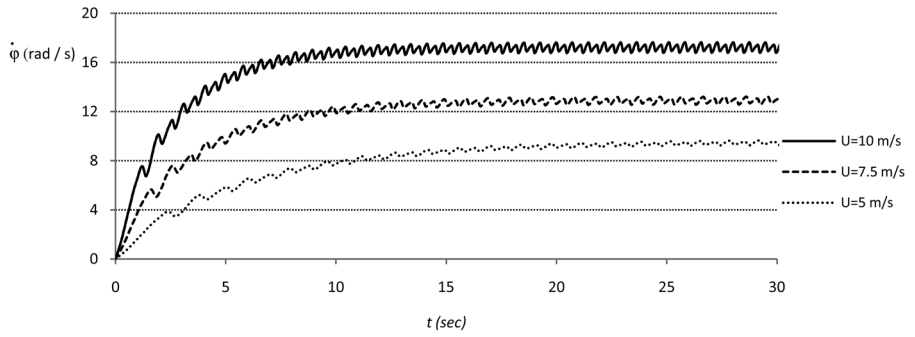

Fig. 11 Time history of angular velocity given by Eq. (7) - small test-sheet, U = 5, 7.5, and 10 m/s

approximately 5% from the models proposed by Iversen and Tachikawa. However, it is noted that Tachikawa's predictions are based on experimental data using thickness parameters τ in the range 0.029 – 0.056 for an aspect ratio A = 1, i.e., lower τ than the actual value for the small test-sheet for the same aspect ratio. The analytical model differs by 15% on average with regard to the experimental data, which suggests that there were important frictional effects at the bearings during the autorotational tests. This difference is due to the fact that the analytical approach has been calibrated through the experimental data considered in Iversen (1979) covering a wide range of aspect ratios, thickness and inertia parameters. As stated in Section 3, the differences observed in the tip velocity, i.e., autorotational periods, for the large test-sheet (cases identified as *L1, L2,* in the table), can be explained in terms of the expected variability for these experiments, as shown in Appendix A.

The dynamic response of the large and small test-sheets computed through the analytical model using $T(\varphi)_{exp}$ is shown in the time domain in Figs. 10 and 11, respectively. It is interesting to observe that the analytical approach seems to have reproduced the asymmetric fluctuation of the angular velocity registered in the experimental data shown in Figs. 4 and 5. This is encouraging since as the analytical model estimates the angular velocity based on the moment coefficients derived from pressure measurements, the corresponding data registered through the gyroscope corresponds to the real motion of the plates.

The fluctuations of the angular velocity $(\dot{\varphi})$ under steady autorotation was measured for the experimental and analytical cases in terms of the index of variation ($I_v = \sigma/\mu$) as defined in Section

Table 3 Index of variation of the angular velocity fluctuation $(d\dot{\varphi})$ under steady autorotation

Case	Large test-sheet			Small test-sheet		
	$U = 5$	$U = 7.5$	$U = 10$	$U = 5$	$U = 7.5$	$U = 10$
I_v - *Experimental*	0.27	0.28	0.31	-	0.10	0.04
I_v - *Analytical*	0.12	0.12	0.12	0.01	0.01	0.01

3. Table 3 shows how this parameter compares for the two test-sheets for every testing velocity. In this case only data for the large test-sheet obtained in the second experiment is presented (no gyroscope was implemented in the experimental work reported in Martinez-Vazquez *et al*. 2009c), whilst only theoretical data for the small test-sheet submitted to $U = 5$ m/s, is provided.

These results suggest that the value of $d\dot{\varphi}$ would ideally be a constant fraction of $\dot{\varphi}$ for the same plate during steady autorotation, i.e., no change with the wind speed. On the other hand, the slope of the initial part of the time series shown in Figs. 10 and 11 suggest that the test-sheets tend to reach the steady autorotation more quickly at higher wind velocities. The differences between the experimental and analytical results could be explained in terms the variability of frictional affects at the bearings. In Schmitz *et al*. (2005), for example, a peak variability of 0.34 times the nominal value was found when misalignment at the bearings was allowed (in that investigation, a variability of 0.02 was determined under controlled conditions). Thus, a variability of 0.25 times the nominal value of steady tip velocity (i.e., about 2/3 of the peak value, see Appendix A), which is higher than the variability found between the analytical (e.g., nominal values) and experimental results shown in Table 3, would be advisable to consider on practical modelling.

4.5 Parametric review

In this section the parametric analysis introduced by Iversen (1979) for the computation of rotational velocity of plates is revisited – which also served to validate the analytical model outlined above. The testing sample in this exercise constitutes 56 plates which include aspect ratios *(A)* and thickness parameters (τ) within the range 0.5 – 4 and 0.0013 – 1.0, respectively. All cases are for an inertia parameter $K = 6.3$ - this value was selected because it tends to the average amongst the experimental data used in Iversen's formulation and also because according to the experimental data presented in Glaser and Northup (1971) the influence of the inertia parameter on the tip velocity is minimal at high values of K. The general characteristics of the 56 plates along with the tip velocity computed through Iversen's and the analytical approaches are given in the Appendix B. It can be inferred from those results that the mean square difference for the predicted tip velocities using both approaches is of the order of 1.5×10^{-4}. This outcome was expected given that the analytical model has been calibrated using Iversen's data. The high degree of precision inferred from this exercise however supports the potential applicability of the analytical method.

The parametric analysis presented in Iversen (1979) can now be extended. Iversen determined the influence of the aspect ratio *(A)* and thickness parameters (τ) in the tip velocity by fitting a curve to relate each of these parameters to experimental data with a thickness parameter $\tau = 0.0325$. Eqs. (7, 9, and 11) have been applied in order to include combinations of A and τ within a range of 1 - 4 and 0.005 - 1, respectively. This is shown in Figs. 12 and 13 whose data correspond to an inertia parameter $K = 6.3$ therefore eq. (2d) must be applied if other values for K are to be considered.

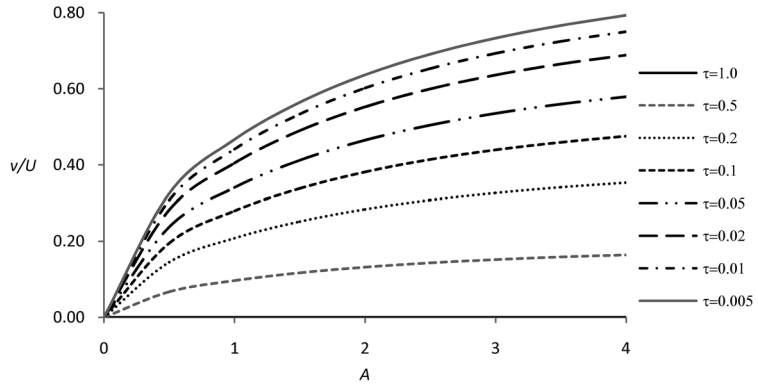

Fig. 12 Influence of aspect ratio *(A)* on $(v / U)_{steady}$, for selected values of τ - analytical method

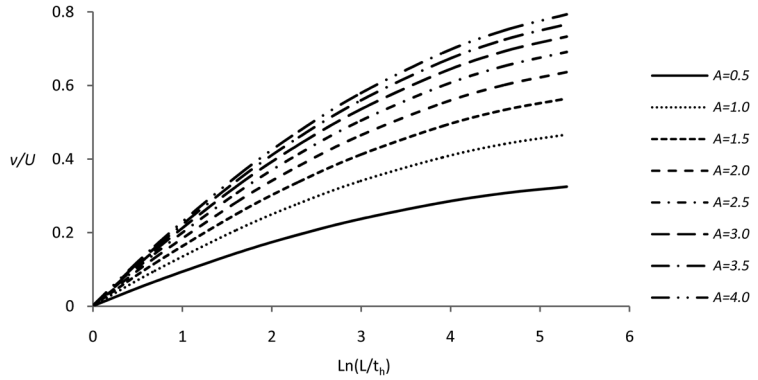

Fig. 13 Influence of the thickness parameter (τ) on $(v / U)_{steady}$, for selected values of A - analytical method

Finally, the tip velocity experimentally determined for the two test-sheets is compared to the corresponding curves inferred from Figs. 12 and 13 for $t = 0.0325$. This is presented in Figs. 14 and 15 where Iversen's curve, used to fit the wind tunnel data from Glaser and Northup (1971), has been reproduced. All data can be represented in the same plot by scaling the experimental results to $\tau = 0.0325$ and $K = 6.3$. In this comparison, the experimental data reported in Martinez-Vazquez *et al*. (2009c) for the large test sheet *(L1)* have been incorporated; *(L2)* and *(sm)* refer to the new experimental data for the large and small test sheet, respectively - note that in these figures the influence of the aspect ratio and thickness parameter on $(v / U)_{steady}$ is presented separately. It can be seen that the experimental values of the tip velocity fall below Iversen's prediction. On average, the difference is 18% although in the particular case of the small board with $U = 7.5$ m/s, a difference of 42% can be observed. From the results shown in table 2 however, in which the tip velocity considers the influence of both the aspect and thickness ratio, a difference of 17% and of 16% is obtained when comparing these results to the Iversen's and Tachikawa methods, respectively. These differences seem to be the result of higher frictional effects at the bearings during autorotational testing than those envisaged by the general formulation of Eqs. (1) and (2).

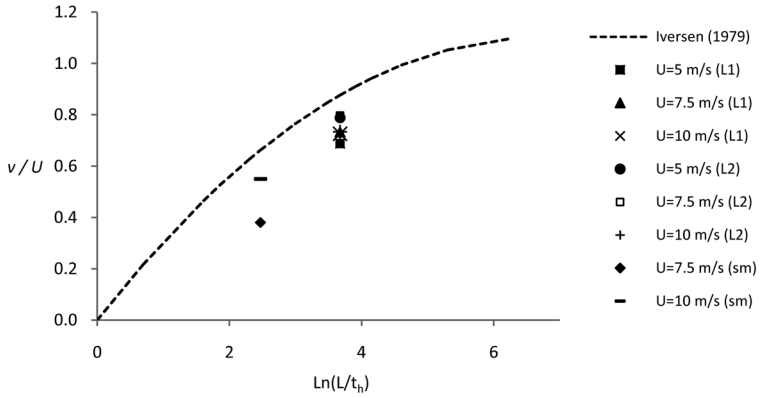

Fig. 14 Comparison between experimental data and Iversen's approach – influence of τ

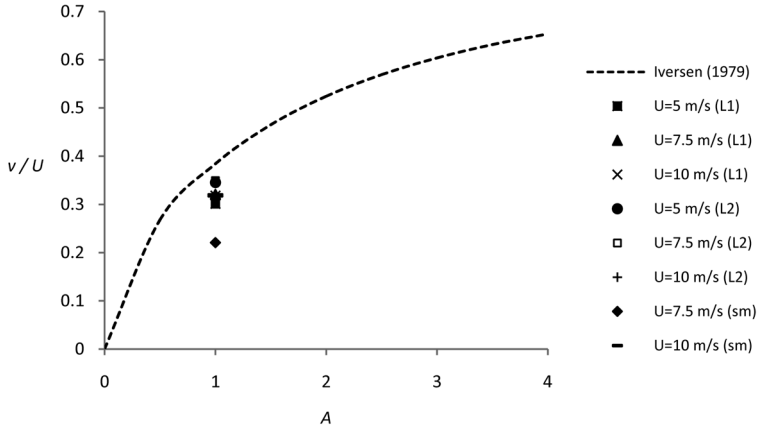

Fig. 15 Comparison between experimental data and Iversen's approach - influence of A

5. Conclusions

A study of autorotational effects on square plates has been presented. Two sets of experimental data involving a large (1 m square) and small (0.3 m square) test-sheet have been described. A comparison of the autorotational periods estimated for the large test sheets using data from both experiments showed differences which have been explained in terms of the variability of the parameters that determine those periods, by using a multivariate estimator where the model parameters, i.e. bearing friction, data processing, etc., were considered as random variables. The central part of the paper was dedicated to the development of an analytical model for estimating tip velocities of autorotating elements. That model it is based on the solution of the equation of angular motion where the frictional effects at the bearings are estimated by using a relatively simple formulation developed in this study. In addition, the moment coefficients derived from the experimental data have been combined with a continuous function proposed by Iversen (1979) thus providing an alternative for estimating the input torque induced by the approaching wind. The analytical method was then used to reproduce the autorotational motion of the two experimental test-sheets, in addition to 56 other cases whose details are given in Appendix B. The overall results

are encouraging. The autorotational motion of the experimental test-sheets, displayed in the time domain, seem to have reproduced the asymmetric fluctuations of the tip velocity found by direct experimentation. Under ideal conditions, those fluctuations would be a constant fraction of the tip velocity, i.e., not changing with variations of the incoming flow. It has also been shown that the analytical results compare fairly well to the simplified approaches proposed by Iversen (1979) and Tachikawa (1983), showing differences of about 5%. The analytical model, as well as Iversen's and Tachikawa's methods report higher tip velocities than those observed in the experiments. Those differences are about 15% on average, which suggests that there were important frictional effects at the bearings during the autorotational tests. One clear example of that was given by the small test-sheet which did not undergo autorotation during the experiments when the wind speed was set to 5 m/s. In that case however, the analytical method, as well as the simplified approaches mentioned above, did predict autorotation for the plate, for a level of friction at the bearings estimated by using the formulation given in this paper.

In the last part of the study, the parametric study presented in Iversen's (1979) was revisited. That study was extended using the analytical method reported in the present investigation. The results have been presented through a series of curves where the separate influence of the aspect ratio and thickness parameters has been shown. Those plots could then be used to obtain a quick estimation of the tip velocity for a wider range of cases. Finally, an overview of the results obtained show that the objectives of the investigation would have been fulfilled, by extending the results obtained by simplified approaches proposed in the past, into the time domain, using new experimental data. The proposed method for simulating time histories opens the possibility of applying spectral or modal techniques that could provide more information about aerodynamic effects on rotational elements.

Acknowledgements

Funding for this research was provided by the United Kingdom's Engineering and Physical Sciences Research Council - grant number EP/F03489X/1. The authors also wish to express their gratitude to Mr. M. Vanderstam of the University of Birmingham for help with the construction of the experimental set.

References

Baker, C.J. (2007), "The debris flight equations", *J. Wind Eng. Ind. Aerod.*, **95**(5), 329-353.

Cohen, M.J. (1976), "Aerodynamics of slender rolling wings at incidence in separated flow", *AIAA J.*, **14**(7), 886-893.

Bustamante, A.G. and Stone G.W. (1969), "The autorotational characteristics of various shapes for subsonic and hypersonic flows", *A.I.A.A.*, 69-132.

Daniels, P. (1970), "A study of the nonlinear rolling motion of a four-finned missile", *J. Spacec. Rocket.*, **7**, 10-512.

Dupleich, P. (1941), "Rotation in free fall of rectangular wings of elongated shape", N. A. C. A., Tech Memo No. 1201.

Flachsbart, O. (1932), "Messungen an ebenen und gewolbten Platten", Ergebnisse der AVA. IV.

Glaser, J.C., Northup, L.L. (1971), "Aerodynamic study of autorotating flat plates", Eng. Res. Inst., Iowa State Univ. Ames, Rep. ISU-ERI-Ames 71037.

Holmes, J.D. (2004), "Trajectories of spheres in strong winds with application to windborne debris", *J. Wind Eng. Ind. Aerod.,* **92**(1), 9-22.
Holmes, J.D., Baker, C.J. and Tamura Y. (2006a), "Tachikawa number: a proposal", *J. Wind Eng. Ind. Aerod*., **94**(1), 41-47.
Holmes, J.D., Letchford, C.W. and Lin, N. (2006b), "Investigation of plate-type windborne debris - Part II. Computed Trajectories", *J. Wind Eng. Ind. Aerod*., **94**(1), 21-39.
Iversen, J.D. (1979), "Autorotating flat-plate wings: the effect of the moment of inertia, geometry and Reynolds number", *J.Fluid Mech*., **92**(2), 327-348.
Kordi, B. and Kopp, A. (2009), "The debris flight equations by C.J. Baker", *J. Wind Eng. Ind. Aerodyn*., **97**, 151-154.
Lin, N., Letchford, C.W. and Holmes, J. D. (2006), "Investigation of plate-type wind borne debris. Part I, Experiments in wind tunnel and full scale", *J. Wind Eng. Ind. Aerod*., **94**(2), 51-76.
Lewis, T.L. and Dods, J.B. (1972), "Wind tunnel measurements of surface pressure fluctuations at mach numbers of 1.6, 2,0, and 2.5, using 12 different transducers", NASA Flight Research Centre, Report No NASA TN D-7087.
Lugt, H. J. (1983), "Autorotation", *Annu. Rev. Fluid Mech.,* **15**, 123-47.
Martinez-Vazquez, P., Baker, C.J., Sterling, M. and Quinn, A.D. (2009a), "The flight of wind borne debris: an experimental analytical and numerical investigation: Part I (Analytical Model)", *Proceedings of the 5th European and African Conference on Wind Engineering (EACWE5)*, Florence, Italy, July.
Martinez-Vazquez, P., Bake,r C.J., Sterling, M., Quinn, A.D. and Richards P.J. (2009b), "The flight of wind borne debris: an experimental analytical and numerical investigation. Part II (Experimental work)", *Proceedings of the 7th Asia-Pacific Conference on Wind Engineering (EACWE7),* Taipei, Taiwan, November.
Martinez-Vazquez, P., Baker, C.J., Sterling, M., Quinn, A.D. and Richards P.J. (2009c), "Aerodynamic forces on fixed and rotating plates", *Wind. Struct.,* **13**(2), 127-144.
Richards, P.J., Williams, N., Laing, B., McCarty, M. and Pond, M. (2008), "Numerical calculation of the 3-Dimensional Motion of Wind-borne Debris", *J. Wind Eng. Ind. Aerod.,* **96**(10-11), 2188-2202.
Schmitz, T.L., Action, J.E. and Ziegert, J.C. and Sawyer W.G. (2005), "The difficulty of measuring low friction: uncertainty analysis for friction coefficient measurements", *J.Tribolt-T. ASME*, **127**(3), 673-678.
Smith, E.H. (1971), "Autorotating wings: an experimental investigation", Univ. Michigan Aerospace Eng. Rep. 01954-2-7.
Tachikawa, M. (1983), "Trajectories of flat plates in uniform flow with application to wind-generated missiles", *J. Wind Eng. Ind. Aerod*., **14**(1-3), 443-453.
Wang, K.J and Letchford, C.W. (2003), "Flight debris behaviour", *Proccedings of the 11th International Conference on Wind Engineering,* Lubbock, Texas, June.
Wills, J.A.B., Lee, B.E. and Wyatt, T.A. (2002), "A model of wind-borne debris damage", *J. Wind Eng. Ind. Aerod.,* **90**(4-5), 555-565.

JH

Appendix A. Variability associated to autorotational periods experimentally determined

The estimation of the autorotational period of a test-sheet using data from wind tunnel experiments can be defined as a multivariate random process. Let $\breve{T} = f\,(I,\ q_E,\ q_L, \gamma,\ d_P)$, where $\breve{T}$ represents the estimated autorotational period, I is the mass moment of inertia with respect to the axis of rotation; q_E and q_L are the static and dynamic pressure during testing, respectively; γ represents the friction at the bearings; and d_P is a factor to take into account the processing of data through the numerical model employed. If $\breve{T}$ is determined from pressure measurements carried out on the same plate, the variation of I would be minimised, however, environmental effects such as

temperature and humidity would still tend to modify the value of I. By considering an extraordinary temperature interval of 30ºC (i.e., from winter to summer) and a coefficient of linear expansion for polystyrene of 8×10^{-5} / (Δ temperature + 273), where temperature is given in ºC, a variation of about 6.5×10^{-5} times the value of I would be obtained, since I depends on the vertical coordinate of every differential of mass, at the second power. On the other hand the water absorption for polystyrene ranges between 0.02 – 0.1 times its volume. By considering an absorption of 0.06 times the total volume, due to humidity, the value of I which depends linearly on the mass of the plate, would vary about 5×10^{-4} times its value. Thus, for the particular case of using the same plate for experimentation, the random variable I would vary about 5.65×10^{-4} times its nominal value.

The wind tunnel equipment used for the present experiment can be divided in two types. The first type corresponds to standard wind tunnel instrumentation. That is the case of a Pitot tube connected to a pressure transducer which was used to obtain the static pressure q_E. In Lewis *et al*. (1972), where a study of 12 different pressure transducers was carried out, a variation of $\pm$ 0.05 was found to represent the accuracy of the group of transducers. That value can be combined with an estimated difference of 1 Pa (i.e., a difference of about 0.04 the nominal reading, on average) between the position of the Pitot tube and the location of the rotating plate, which were approximately 2 m apart from each other. A variation of 0.09 times the static pressure seems thus appropriate for taking into account the variability of q_E. The second type of experimental equipment, associated to the random variable q_L, corresponds to the on-board logging system formed by pressure transducers connected to portable data loggers. The sensors provide 12-bit resolution, which over a range of 4 V would introduce an error of about 9.7×10^{-4} V, whilst a variation of about 0.0025 V would have been introduced by fluctuations in the power supplied by the potable logger. In addition, a variation of about $\pm$ 10 mV would be due to a long term drift, once the two experiments reported in this paper were carried out within a period of time of approximately 6 months. Altogether, there would be a variation for q_L of about 0.013 V, i.e., 0.0034 times the range of voltage under operation (4 V). In the case of the friction (γ), the most common errors in estimating it value are caused by misalignments in the bearing system - see for example Schmitz *et al*. (2005). Friction variations would also include changes in the viscosity of the lubricant, type of bearing material, etc. In that paper, a lower limit of 0.02 times the nominal friction was found when the sources of error were minimised, whilst a peak value of 0.34 was reported by allowing misalignment. Thus, a variation of 0.25 times the nominal value of γ, appears to be adequate, i.e., about 2/3 of the peak value. Finally, the model for processing experimental data would introduce some variability for d_P. In Rojiani *et al*. (1981), a coefficient of variation of 0.10, defined as σ / μ, where σ, μ represent *rms* and mean value, respectively, is considered for a model for structural analysis. In analogy to that, even though the differences between a structural model and the method for determining the rotational period adopted in the investigation, an error proportional to two standard deviations, i.e., 0.20 times the nominal value (for example μ) will be adopted for d_P. The reason of considering two standard deviations is that, the variability associated to the rest of the parameters has been done over the basis that these are peak values.

The proportional influence of every random variable in the estimation of $\check{T}$ will not be determined here. In the case of an equally linear influence form all variables, we have then that the variation in the autorotational period of the test-sheet (using the same specimen) would be of about $\Delta \check{T} = [(5.65 \times 10^{-4})^2 + (0.09)^2 + (0.0034)^2 + (0.25)^2 + (0.2)^2]^{1/2} = 0.332$. The corresponding coefficient of variation, as defined above, would then be 0.1662.

Appendix B. Tip velocity predicted for various plates – Iversen's and Proposed Method

Table B1 Estimation of $(v / U)_{steady}$ using Iversen's approach and the proposed analytical model

case	b (m)	L (m)	t (m)	ρ (kg/m^3)	A	τ	K	m (kg)	D_0	$(v / U)_{steady}$	$(v / U)_{steady}$
#									Kg-m^2/rad-s	Eqs. (7,9,11)	Eq. (2)
1	0.25	0.50	0.005	9261.0	0.50	0.0100	6.30	5.8	0.0178	0.2992	0.3072
2	0.25	0.50	0.010	4630.5	0.50	0.0200	6.30	5.8	0.0194	0.2684	0.2821
3	0.25	0.50	0.020	2315.3	0.50	0.0400	6.30	5.8	0.0219	0.2374	0.2494
4	0.25	0.50	0.050	926.1	0.50	0.1000	6.30	5.8	0.0280	0.1853	0.1948
5	0.25	0.50	0.100	463.1	0.50	0.2000	6.30	5.8	0.0377	0.1376	0.1448
6	0.25	0.50	0.200	231.5	0.50	0.4000	6.30	5.8	0.0625	0.0820	0.0874
7	0.25	0.50	0.500	92.6	0.50	1.0000	6.30	5.8	0.0000	0.0000	0.0000
8	1.00	1.00	0.005	18522.0	1.00	0.0050	6.30	92.6	0.1874	0.4395	0.4663
9	1.00	1.00	0.010	9261.0	1.00	0.0100	6.30	92.6	0.1983	0.4164	0.4409
10	1.00	1.00	0.020	4630.5	1.00	0.0200	6.30	92.6	0.2160	0.3836	0.4047
11	1.00	1.00	0.050	1852.2	1.00	0.0500	6.30	92.6	0.2567	0.3237	0.3405
12	1.00	1.00	0.100	926.1	1.00	0.1000	6.30	92.6	0.3128	0.2662	0.2795
13	1.00	1.00	0.200	463.1	1.00	0.2000	6.30	92.6	0.4207	0.1978	0.2078
14	1.00	1.00	0.500	185.2	1.00	0.5000	6.30	92.6	0.9052	0.0918	0.0966
15	2.25	1.50	0.005	27783.0	1.50	0.0033	6.30	468.8	0.7679	0.5477	0.5763
16	2.25	1.50	0.010	13891.5	1.50	0.0067	6.30	468.8	0.8001	0.5236	0.5531
17	2.25	1.50	0.020	6945.8	1.50	0.0133	6.30	468.8	0.8561	0.4919	0.5169
18	2.25	1.50	0.050	2778.3	1.50	0.0333	6.30	468.8	0.9851	0.4277	0.4492
19	2.25	1.50	0.100	1389.2	1.50	0.0667	6.30	468.8	1.1556	0.3646	0.3830
20	2.25	1.50	0.200	694.6	1.50	0.1333	6.30	468.8	1.4568	0.2892	0.3038
21	2.25	1.50	0.500	277.8	1.50	0.3333	6.30	468.8	2.4696	0.1706	0.1792
22	4.00	2.00	0.005	37044.0	2.00	0.0025	6.30	1481.8	2.1308	0.6516	0.6564
23	4.00	2.00	0.010	18522.0	2.00	0.0050	6.30	1481.8	2.1982	0.6335	0.6363
24	4.00	2.00	0.020	9261.0	2.00	0.0100	6.30	1481.8	2.3251	0.6005	0.6015
25	4.00	2.00	0.050	3704.4	2.00	0.0250	6.30	1481.8	2.6230	0.5230	0.5332
26	4.00	2.00	0.100	1852.2	2.00	0.0500	6.30	1481.8	3.0105	0.4642	0.4646
27	4.00	2.00	0.200	926.1	2.00	0.1000	6.30	1481.8	3.6676	0.3842	0.3813
28	4.00	2.00	0.500	370.4	2.00	0.2500	6.30	1481.8	5.6193	0.2513	0.2489
29	6.25	2.50	0.005	46305.0	2.50	0.0020	6.30	3617.6	4.7677	0.7205	0.7162
30	6.25	2.50	0.010	23152.5	2.50	0.0040	6.30	3617.6	4.8818	0.7026	0.6994
31	6.25	2.50	0.020	11576.3	2.50	0.0080	6.30	3617.6	5.1204	0.6712	0.6668
32	6.25	2.50	0.050	4630.5	2.50	0.0200	6.30	3617.6	5.6963	0.6043	0.5994

Table B1 Estimation of $(v / U)_{steady}$ using Iversen's approach and the proposed analytical model

case	b (m)	L (m)	t (m)	ρ (kg/m^3)	A	τ	K	m (kg)	D_0	$(v / U)_{steady}$	$(v / U)_{steady}$
#									Kg-m^2/rad-s	Eqs. (7,9,11)	Eq. (2)
33	6.25	2.50	0.100	2315.3	2.50	0.0400	6.30	3617.6	6.4422	0.5343	0.5300
34	6.25	2.50	0.200	1157.6	2.50	0.0800	6.30	3617.6	7.6770	0.4485	0.4448
35	6.25	2.50	0.500	463.1	2.50	0.2000	6.30	3617.6	11.0952	0.3100	0.3077
36	9.00	3.00	0.005	55566.0	3.00	0.0017	6.30	7501.4	9.2950	0.7615	0.7617
37	9.00	3.00	0.010	27783.0	3.00	0.0033	6.30	7501.4	9.4606	0.7480	0.7484
38	9.00	3.00	0.020	13891.5	3.00	0.0067	6.30	7501.4	9.8578	0.7193	0.7183
39	9.00	3.00	0.050	5556.6	3.00	0.0167	6.30	7501.4	10.8500	0.6556	0.6526
40	9.00	3.00	0.100	2778.3	3.00	0.0333	6.30	7501.4	12.1372	0.5872	0.5834
41	9.00	3.00	0.200	1389.2	3.00	0.0667	6.30	7501.4	14.2367	0.5010	0.4973
42	9.00	3.00	0.500	555.7	3.00	0.1667	6.30	7501.4	19.7891	0.3608	0.3578
43	12.25	3.50	0.005	64827.0	3.50	0.0014	6.30	13897.3	16.4564	0.7835	0.7971
44	12.25	3.50	0.010	32413.5	3.50	0.0029	6.30	13897.3	16.6662	0.7835	0.7871
45	12.25	3.50	0.020	16206.8	3.50	0.0057	6.30	13897.3	17.2723	0.7321	0.7594
46	12.25	3.50	0.050	6482.7	3.50	0.0143	6.30	13897.3	18.8481	0.6827	0.6959
47	12.25	3.50	0.100	3241.4	3.50	0.0286	6.30	13897.3	20.9041	0.6212	0.6275
48	12.25	3.50	0.200	1620.7	3.50	0.0571	6.30	13897.3	24.2254	0.5419	0.5415
49	12.25	3.50	0.500	648.3	3.50	0.1429	6.30	13897.3	32.7315	0.4036	0.4008
50	16.00	4.00	0.005	74088.0	4.00	0.0013	6.30	23708.2	27.1257	0.8105	0.8250
51	16.00	4.00	0.010	37044.0	4.00	0.0025	6.30	23708.2	27.3538	0.8050	0.8181
52	16.00	4.00	0.020	18522.0	4.00	0.0050	6.30	23708.2	28.2189	0.7808	0.7930
53	16.00	4.00	0.050	7408.8	4.00	0.0125	6.30	23708.2	30.5741	0.7277	0.7319
54	16.00	4.00	0.100	3704.4	4.00	0.0250	6.30	23708.2	33.6722	0.6643	0.6646
55	16.00	4.00	0.200	1852.2	4.00	0.0500	6.30	23708.2	38.6467	0.5803	0.5790
56	16.00	4.00	0.500	740.9	4.00	0.1250	6.30	23708.2	51.0886	0.4413	0.4380